

Mechanism of enhanced luminescence in $\text{In}_x\text{Al}_y\text{Ga}_{1-x-y}\text{N}$ quaternary epilayers

C. H. Chen and Y. F. Chen

Department of Physics, National Taiwan University, Taipei, Taiwan, Republic of China

Z. H. Lan, L. C. Chen, and K. H. Chen

Center for Condensed Matter Sciences, National Taiwan University, Taipei, Taiwan, Republic of China

H. X. Jiang and J. Y. Lin

Department of Physics, Kansas State University, Manhattan, Kansas 6506-2601

(Received 14 July 2003; accepted 29 December 2003)

We report firm evidence for the underlying mechanism of the enhanced luminescence in $\text{In}_x\text{Al}_y\text{Ga}_{1-x-y}\text{N}$ quaternary epilayers. Photoluminescence, Raman scattering, field emission scanning electron microscopy (SEM), energy dispersive x-ray spectrometry (EDS), and cathodoluminescence (CL) measurements have been employed to study the correlation between optical and structural properties in these alloys. The phonon replica structures accompanying luminescence line, InGaN-related phonon modes in Raman spectra, SEM images, element composition analysis by EDS, and localized CL spectra provide the evidence to show that the existence of InGaN-like nanoclusters is responsible for the enhanced luminescence in $\text{In}_x\text{Al}_y\text{Ga}_{1-x-y}\text{N}$ quaternary alloys. Our result therefore gives an excellent demonstration showing that because of the existence of nanoclusters a very defective alloy can exhibit a strong emission even at room temperature. © 2004 American Institute of Physics. [DOI: 10.1063/1.1650549]

The group III-nitride wide-band-gap semiconductors have been recognized as very important materials for many optoelectronic devices, such as blue ultraviolet (UV) light emitting diodes (LEDs), laser diodes (LDs), and high-temperature/high-power electronic devices.¹⁻³ Even though the nitride LEDs and LDs have been commercialized, the exact mechanism that can overcome high dislocation density and give strong emission is still unclear. It has been demonstrated that most nitride based devices must take advantage of multiple quantum wells (MQWs) and heterostructures such as GaN/AlGaIn^{4,5} and InGaN/GaN⁶⁻⁸ as well as the tunability of the band gaps in the alloys from InN (1.9 eV) to GaN (3.4 eV) and to AlN (6.2 eV). Recently, $\text{In}_x\text{Al}_y\text{Ga}_{1-x-y}\text{N}$ quaternary alloys have also been recognized to have the potential to overcome some shortfall of GaN epilayers, InGaN, and AlGaIn alloys.¹⁻⁸ By varying In and Al compositions x and y in $\text{In}_x\text{Al}_y\text{Ga}_{1-x-y}\text{N}$, one can change the energy band gap while keeping lattice matched with GaN, which can be used to reduce dislocation density as well as piezoelectric field. In addition to the key features of lattice match with GaN and tunability in energy band gap, $\text{In}_x\text{Al}_y\text{Ga}_{1-x-y}\text{N}$ quaternary alloys also have the potential to provide a better thermal match to GaN, which could be an important advantage in epitaxial growth. The potential application of $\text{In}_x\text{Al}_y\text{Ga}_{1-x-y}\text{N}$ quaternary alloys as InGaN/InAlGaIn quantum well light emitters,⁹ GaN/InAlGaIn heterojunction field-effect transistors,¹⁰ and UV detectors have been demonstrated recently.¹¹ Similar to the strong emission in InGaN alloys, it was also found that the quantum efficiency of $\text{In}_x\text{Al}_y\text{Ga}_{1-x-y}\text{N}$ is enhanced significantly over AlGaIn with a comparable Al content.¹² The enhanced luminescent efficiency has been attributed to the existence of alloy clusters,¹³ but it lacks direct evidence. In this letter, we simultaneously perform both structural and optical studies including photoluminescence (PL), Raman, field emission

scanning electron microscopy (SEM) image, energy dispersive X-ray spectrometry (EDS), and cathodoluminescence (CL) measurements. We clearly observe the existence of nanoclusters in $\text{In}_x\text{Al}_y\text{Ga}_{1-x-y}\text{N}$ quaternary alloys from SEM images, resolve the local composition by EDS measurement, and distinguish the luminescence spectra taken in the regions inside and outside of a nanocluster. Together with the studies of fine structures in PL and Raman spectra, we firmly establish that the existence of InGaN-like nanoclusters is responsible for the enhanced luminescence in $\text{In}_x\text{Al}_y\text{Ga}_{1-x-y}\text{N}$ epilayers. Our results shown here provide concrete evidence to resolve the long-standing puzzle in nitride semiconductor, in which a defective alloy can have a strong emission even at room temperature.

A set of $\text{In}_x\text{Al}_y\text{Ga}_{1-x-y}\text{N}$ quaternary alloys with different Al concentration has been grown by metalorganic chemical vapor deposition (MOCVD). A 1.0 μm GaN epilayer was first deposited on the sapphire substrate with 25 nm low temperature GaN buffer layer, followed by the deposition of 0.1 μm $\text{In}_x\text{Al}_y\text{Ga}_{1-x-y}\text{N}$ quaternary alloy epilayer by the low pressure MOCVD. The growth temperature and pressure for the underneath GaN epilayer were 1050 °C and 300 Torr, respectively. For $\text{In}_x\text{Al}_y\text{Ga}_{1-x-y}\text{N}$ quaternary alloys, the growth temperature 780 °C and In and Al compositions were controlled by varying the flow rates of TMIIn and TMAI. Contents of In and Al were determined by different methods including x-ray diffraction (XRD), energy dispersive system, and Rutherford backscattering.¹² It was found that $\text{In}_x\text{Al}_y\text{Ga}_{1-x-y}\text{N}$ quaternary alloys, which are lattice matched with GaN epilayers ($y \sim 4.8x$, which is very close to the theoretical value), have the highest PL intensity as well as the narrowest XRD linewidth. The XRD linewidth is approximately equal to 1000 arcsec.

The PL spectra were recorded by a SPEX 0.85 m double spectrometer, and a photomultiplier tube. The sample was

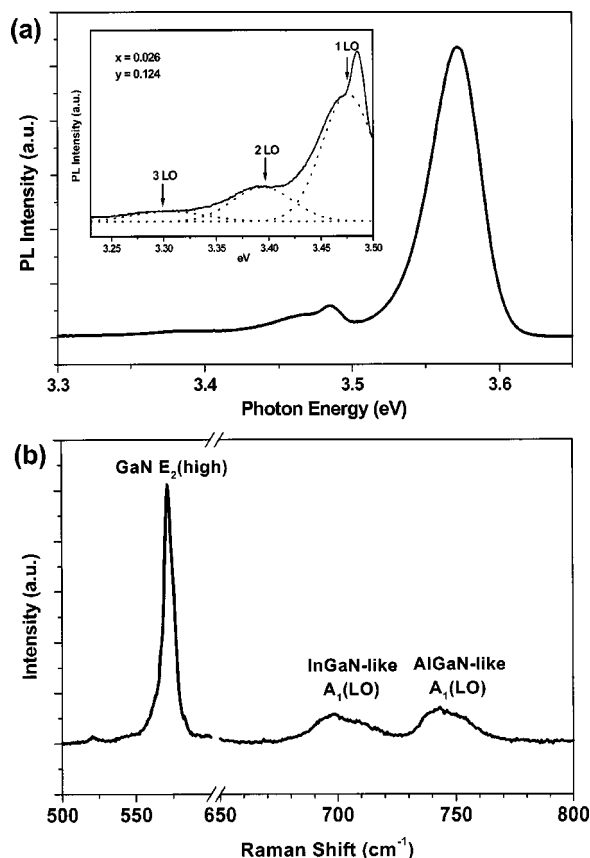


FIG. 1. (a) Photoluminescence spectra of the $\text{In}_x\text{Al}_y\text{Ga}_{1-x-y}\text{N}$ quaternary alloys at temperature of 15 K. In the inset, the enlarged photoluminescence spectrum of lattice-matched sample was fitted by Gaussian curves (dot lines). By the fitting result, the energy of LO-phonon replicas is 86 meV. (b) Room-temperature micro-Raman spectra of the $\text{In}_x\text{Al}_y\text{Ga}_{1-x-y}\text{N}$ quaternary alloy samples probed with a solid-state laser (532 nm).

placed inside a closed-cycle He cryostat. A He–Cd laser working at 325 nm was used as the excitation source. The Raman signal was measured by a Jobin-Yvon T64000 Micro-Raman system working in the triple subtractive mode. The Raman spectra of the samples were measured at room temperature using a solid-state laser with a 532 nm wavelength, and they were measured in backscattering geometry. The incident and scattered light propagated parallel to the c axis, which in turn was normal to the growth surface. The SEM images were taken by using a field emission SEM (JEOL JSM-6700F) electron microscopy. The e-beam resolution is about 10 nm and the radius of diffusive region in the sample is about 30–40 nm. EDS measurements were performed with the same field emission SEM operated at 15 kV with a probe diameter of 1 nm. The CL measurement used a commercial MonoCL3 of Gatan. Here, the light is collected by a paraboloidal collecting mirror and directed onto a monochromator and detected by a cooled photomultiplier tube.

Figure 1(a) shows the PL spectrum of the $\text{In}_x\text{Al}_y\text{Ga}_{1-x-y}\text{N}$ quaternary alloy with $x=0.026$ and $y=0.124$ at temperature 15 K. The PL spectrum is dominated by a sharp emission and full width at half maximum is about 34 meV. The lower emission peak at 3.483 eV is due to the underneath GaN epilayer. We found not only a higher emission energy but also higher emission intensity in $\text{In}_x\text{Al}_y\text{Ga}_{1-x-y}\text{N}$ quaternary alloys than that of high quality GaN epilayer.¹² Its quantum efficiency is comparable to that

of InGaN alloys and is significantly over AlGaN with a similar Al content.¹² Several phonon replicas can be clearly observed on the low energy shoulder of the main PL peak. As shown in the inset of Fig. 1(a), we took a multi-Gaussian fit of the PL line, and we found that the separation between adjacent peaks is about 86 meV, which is in excellent agreement with the InGaN-like LO phonon energy measured by Raman scattering as shown in Fig. 1(b). This result strongly implies that the InGaN-like regions do exist in the $\text{In}_x\text{Al}_y\text{Ga}_{1-x-y}\text{N}$ matrix, and the electron–hole pairs responsible for the bright luminescence in $\text{In}_x\text{Al}_y\text{Ga}_{1-x-y}\text{N}$ quaternary alloys are confined in the InGaN-like region. Because the electron–hole pairs are confined in InGaN-like clusters, which enhance the wave function overlap and thus the transition probability, the $\text{In}_x\text{Al}_y\text{Ga}_{1-x-y}\text{N}$ alloys therefore can overcome the influence of a large number of defects and provide the bright emission. In addition, due to the confinement of electron–hole pairs in InGaN-like regions, there will be a strong interaction between electron–hole pairs and InGaN-like lattice. Therefore, the PL spectra display the InGaN-like phonon replicas. In Fig. 1(b), we showed the room-temperature Raman spectra of $\text{In}_x\text{Al}_y\text{Ga}_{1-x-y}\text{N}$ quaternary alloys. There are three resolved phonon structures observed in each Raman spectrum of $\text{In}_x\text{Al}_y\text{Ga}_{1-x-y}\text{N}$ quaternary alloys. The 569 cm^{-1} peak is from E_2 mode of h-GaN. The broaden line in 696 cm^{-1} is the InGaN-like A_1 (LO) mode and that in 745 cm^{-1} is AlGaN-like A_1 (LO) mode. The above assignment of both InGaN-like A_1 mode and AlGaN-like A_1 mode is based on the energy of GaN A_1 (LO) phonon^{14,15} at 735 cm^{-1} and the phonon modes of InGaN and AlGaN alloys given in previous reports.^{16–18} Thus, this finding provides excellent evidence to support the existence of InGaN-like clusters in $\text{In}_x\text{Al}_y\text{Ga}_{1-x-y}\text{N}$ quaternary alloys. Moreover, the energy of the InGaN-related A_1 (LO) obtained in Raman spectra is consistent with that obtained from PL spectrum. Therefore, the excellent correlation between PL and Raman spectra strongly suggests that the electron–hole pairs responsible for the enhanced emission in $\text{In}_x\text{Al}_y\text{Ga}_{1-x-y}\text{N}$ alloys are confined in InGaN-like regions.

In order to provide more direct evidence for the above-described model, we have performed SEM image and EDS measurements. Figure 2(a) shows the SEM micrograph of the $\text{In}_x\text{Al}_y\text{Ga}_{1-x-y}\text{N}$ quaternary alloy with $x=0.026$ and $y=0.124$. Indeed, nanoclusters with a dark contrast are clearly observed. Typical dimensions of nanoclusters are in the range of 10–100 nm. The density of these dots is about 10^{13} cm^{-2} . To spatially resolve the composition in different regions, we have also performed EDS measurements for inside and outside of a nanocluster as shown in Fig. 2(b). From EDS measurements, the In and Al compositions in the center of the nanocluster can be estimated, which are larger and smaller, respectively, than those outside of the nanocluster. Therefore, we can find that the nanoclusters observed in SEM images are InGaN-rich regions. This provides direct evidence for the formation of InGaN-like nanoclusters in $\text{In}_x\text{Al}_y\text{Ga}_{1-x-y}\text{N}$ matrix. However, it is worth noting that the difference in In/Al composition measured inside and outside cluster is not large. We believe that this result is due to the resolution limitation of EDS technique. The EDS measure-

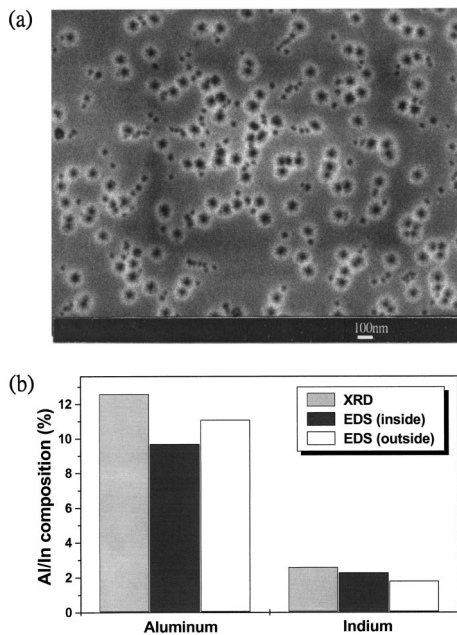


FIG. 2. (a) SEM image of the $\text{In}_x\text{Al}_y\text{Ga}_{1-x-y}\text{N}$ quaternary alloys. (b) Indium and aluminum composition at different nanoregions determined by EDS data.

ment can only tell us the qualitative difference of the composition.

To obtain the spatially resolved optical properties, we have focused the electron beam on a single cluster and measure the CL spectra. The local spectra taken inside and outside regions of a nanocluster are shown in Fig. 3. The CL spectrum taken inside the nanocluster is in excellent agreement with the main peak of the PL spectra shown in Fig. 1(a). This result indicates that InGaN-like nanoclusters are indeed responsible for the enhanced luminescence in $\text{In}_x\text{Al}_y\text{Ga}_{1-x-y}\text{N}$ epilayers. When going from inside toward outside region of the nanocluster, the CL spectra becomes blueshifted, weak, and broad. This behavior can be well understood according to the formation of InGaN-like nanoclusters. Because the indium-rich region has a small bandgap, the photoexcited electron-hole pairs are easily accumulated and confined in InGaN-like nanoclusters. It leads to the enhancement of the wave function overlap as well as transition probability. In addition, the confined electron-hole pairs are beneficial for radiative recombination, because they have less probability to diffuse to nonradiative recombination centers. The CL spectrum of the region inside nanoclusters thus have

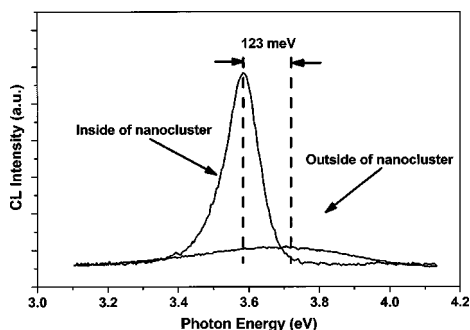


FIG. 3. Local CL spot spectra of $\text{In}_x\text{Al}_y\text{Ga}_{1-x-y}\text{N}$ quaternary alloys taken in the regions inside and outside of a nanocluster. The CL intensity has been normalized for the illumination area.

higher intensity and narrower linewidth. For the regions outside nanoclusters, the electron-hole pairs are not confined, and they can diffuse randomly. Before making a radiative recombination, they can interact with crystal defects such as alloy disorder and dislocations. The CL spectrum will reflect the crystal quality, which is thus broad and weak. This is the spectrum that one should expect intuitively for a defective quaternary alloy without the existence of nanoclusters. Besides, because the Al composition is higher in this region, the CL spectrum is blueshifted. The result shown here therefore provides an excellent model system for the underlying mechanism of the enhanced luminescence in nitride semiconductors. It can be used to resolve the long-standing puzzle in which a defect-rich alloy can have a strong emission at room temperature.

In conclusion, the spatial correlation of the enhanced luminescence in $\text{In}_x\text{Al}_y\text{Ga}_{1-x-y}\text{N}$ quaternary epilayers has been investigated. The phonon replica structures accompanying luminescence line, InGaN-related phonon modes in Raman spectra, SEM images, element composition analysis by EDS, and localized CL spectra provide the evidence to support the fact that the formation of nanoclusters is responsible for the enhanced luminescence in $\text{In}_x\text{Al}_y\text{Ga}_{1-x-y}\text{N}$ quaternary alloys. Therefore, our result shown here can serve as an excellent model system to demonstrate that a rather defective alloy can exhibit a strong emission even at room temperature because of the existence of nanoclusters.

This work was partly supported by the National Science Council and Ministry of Education of the Republic of China.

- ¹M. A. Khan, A. Bhattarai, J. N. Kuznia, and D. T. Olson, *Appl. Phys. Lett.* **63**, 1214 (1993).
- ²H. Morkoc, S. Strite, G. B. Gao, M. E. Lin, B. Sverdlov, and M. Burns, *J. Appl. Phys.* **76**, 1363 (1994).
- ³S. Nakamura, M. Senoh, S. Nagahama, N. Iwasa, T. Yamada, T. Matsushita, H. Kiyoko, and Y. Sugimoto, *Jpn. J. Appl. Phys., Part 2* **35**, L74 (1996).
- ⁴C. H. Chen, Y. F. Chen, An Shih, S. C. Chen, and H. X. Jiang, *Appl. Phys. Lett.* **78**, 3035 (2001).
- ⁵D. R. Hang, C. H. Chen, Y. F. Chen, H. X. Jiang, and J. Y. Lin, *J. Appl. Phys.* **90**, 1887 (2001).
- ⁶Y. Narukawa, Y. Kawakami, M. Funato, S. Fujita, S. Fujita, and S. Nakamura, *Appl. Phys. Lett.* **70**, 981 (1997).
- ⁷S. Chichibu, T. Azuhata, T. Sota, and S. Nakamura, *Appl. Phys. Lett.* **70**, 2822 (1997).
- ⁸H. C. Yang, P. F. Kuo, T. Y. Lin, Y. F. Chen, K. H. Chen, L. C. Chen, and J.-I. Chyi, *Appl. Phys. Lett.* **76**, 3712 (2000).
- ⁹M. E. Aumer, S. F. LeBoeut, S. M. Bedair, M. Smith, J. Y. Lin, and H. X. Jiang, *Appl. Phys. Lett.* **77**, 821 (2000).
- ¹⁰M. A. Khan, J. W. Yang, G. Simin, R. Gaska, M. S. Shur, G. Tamulaitis, A. Zukauskas, D. J. Smith, D. Chandrasekhar, and R. Bicknell-Tassius, *Appl. Phys. Lett.* **76**, 1161 (2000).
- ¹¹T. N. Oders, J. Li, J. Y. Lin, and H. X. Jiang, *Appl. Phys. Lett.* **77**, 791 (2000).
- ¹²J. Li, K. B. Nam, K. H. Kim, J. Y. Lin, and H. X. Jiang, *Appl. Phys. Lett.* **78**, 61 (2001).
- ¹³C. H. Chen, L. Y. Huang, Y. F. Chen, H. X. Jiang, and J. Y. Lin, *Appl. Phys. Lett.* **80**, 1397 (2002).
- ¹⁴H. Siegle, G. Kaczmarczyk, L. Filippidis, A. P. Litvinchuk, A. Hoffmann, and C. Thomsen, *Phys. Rev. B* **55**, 7000 (1997).
- ¹⁵G. Wei, J. Zi, K. Zhang, and X. Xie, *J. Appl. Phys.* **82**, 4693 (1997).
- ¹⁶J. Wagner, A. Ramakrishnan, H. Obloh, and M. Maier, *Appl. Phys. Lett.* **74**, 3863 (1999).
- ¹⁷D. Behr, R. Niebuhr, J. Wagner, K.-H. Bachem, and U. Kaufmann, *Appl. Phys. Lett.* **70**, 363 (1997).
- ¹⁸F. Demangeot, J. Groenen, J. Frandon, M. A. Renucci, O. Briot, S. Clur, and R. L. Aulombard, *Appl. Phys. Lett.* **72**, 2674 (1998).